

Universitat de Lleida

Document downloaded from:

<http://hdl.handle.net/10459.1/60525>

The final publication is available at:

<https://doi.org/10.1016/j.est.2017.11.002>

Copyright

cc-by-nc-nd, (c) Elsevier, 2017



Està subjecte a una llicència de [Reconeixement-NoComercial-SenseObraDerivada 4.0 de Creative Commons](https://creativecommons.org/licenses/by-nc-nd/4.0/)

1 Enthalpy-temperature plots to compare calorimetric measurements of 2 phase change materials at different sample scales

3 Christoph Rathgeber ^{a,*}, Henri Schmit ^a, Laia Miró ^b, Luisa F. Cabeza ^b, Andrea Gutierrez ^{1c},
4 Svetlana N. Ushak ^c, Stefan Hiebler ^a

5
6
7 ^aBavarian Center for Applied Energy Research – ZAE Bayern, Walther-Meissner-Str. 6,
8 85748 Garching, Germany

9 ^bGREA Innovació concurrent, INSPIRES Research Centre, University of Lleida, Pere de Cabrera s/n,
10 25001 Lleida, Spain

11 ^cUniversity of Antofagasta and Center for Advanced Study of Lithium and Industrial Minerals
12 (CELiMIN), Campus Coloso, Av. Universidad de Antofagasta 02800, Antofagasta, Chile

13
14 *Corresponding author. *Tel.*: +49 8932944288. *E-mail address*: christoph.rathgeber@zae-bayern.de
15

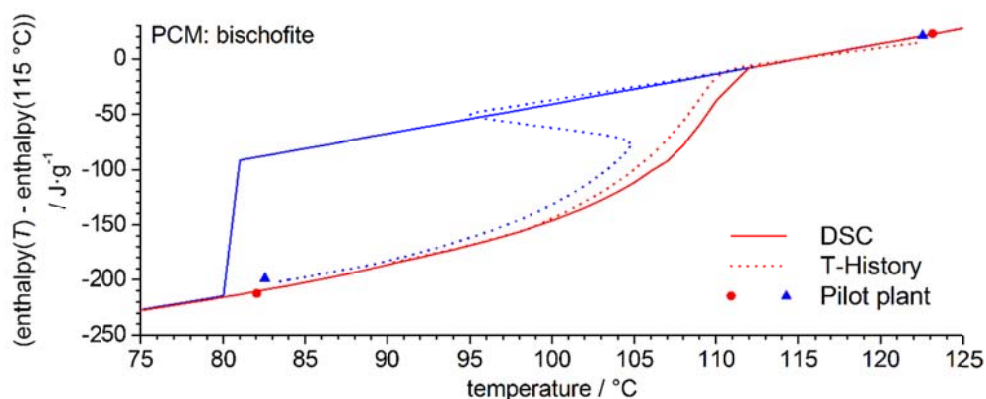
16 *Highlights*

- 17 • Four PCM were investigated (RT58, bischofite, D-mannitol, and hydroquinone).
- 18 • Measurements at three scales (DSC, T-History, and pilot plant) were carried out.
- 19 • Sample volumes are ~15 µl (DSC), ~15 ml (T-History), and ~150 l (pilot plant).
- 20 • Tabular enthalpy changes within defined temperature ranges are difficult to compare.
- 21 • Enthalpy-temperature plots facilitate the interpretation of measured results.

22
23
24
25
26
27
28
29

¹ Present affiliation: German Aerospace Center – DLR e.V., Institute of Technical Thermodynamics, Pfaffenwaldring 38, 70569 Stuttgart, Germany

30 *Graphical abstract*



31

32

33

34 **Abstract**

35 Phase change materials (PCM) can provide high thermal energy storage capacities in narrow
36 temperature ranges around their phase change temperature. The expectable maximum storage capacity
37 of a PCM in a defined temperature range is equal to the enthalpy change in that range and can be
38 determined via calorimetric measurements such as differential scanning calorimetry (DSC) or
39 T-History calorimetry. T-History samples (~15 ml) are about 1000 times larger than DSC samples
40 (~15 μ l). Experiments in a pilot plant are performed to study the charging and discharging behaviour
41 of even larger amounts of the PCM (~150 l). The common practise is to investigate PCM at one scale,
42 rarely at two scales. In this work, the characterisation was carried out at three scales (DSC, T-History,
43 and pilot plant) for four PCM (RT58, bischofite, D-mannitol, and hydroquinone). Thereby, the
44 question arises how the enthalpy changes measured at different scales and under different conditions
45 can be compared. In literature, the melting enthalpy is usually assigned to a single temperature without
46 indicating the temperature range considered for evaluation. In very few instances, the enthalpy change
47 within a defined temperature range is stated. In both cases, results measured under different conditions
48 are difficult to compare. In this work, it is demonstrated that enthalpy-temperature plots facilitate the
49 comparison and interpretation of measurements obtained under different experimental methods at
50 different sample scales.

51

52 *Keywords:*

53 Thermal energy storage (TES); Latent heat storage; Phase change material (PCM); Storage capacity;

54 Enthalpy curve; T-History

55

56 *Nomenclature:*

57 $h(T)$ mass-specific enthalpy curve/ $J \cdot g^{-1}$

58 $\Delta h_{\Delta T_c}$ mass-specific enthalpy change upon crystallisation within $\Delta T_c/J \cdot g^{-1}$

59 $\Delta h_{\Delta T_m}$ mass-specific enthalpy change upon melting within $\Delta T_m/J \cdot g^{-1}$

60 T_{in} inlet temperature for measurements at pilot plant scale/ $^{\circ}C$

61 T_m melting temperature/ $^{\circ}C$

62 T_{PCM} PCM temperature during measurements at pilot plant scale/ $^{\circ}C$

63 ΔT_c temperature interval for the determination of $\Delta h_{\Delta T_c}/K$

64 ΔT_m temperature interval for the determination of $\Delta h_{\Delta T_m}/K$

65

66 *Abbreviations:*

67 AHE air-HTF heat exchanger

68 DSC differential scanning calorimetry

69 HTF heat transfer fluid

70 PCM phase change material

71 TES thermal energy storage

72

73 **1. Introduction**

74 Thermal energy storage using phase change materials (PCM) provides high storage capacities in
75 narrow temperature ranges. Most of the PCM used in applications are solid-liquid PCM storing heat or
76 cold in repeated melting and crystallisation processes [1]-[3]. To select a suitable PCM for an
77 application, the entire phase change has to take place within the temperature interval of the application.
78 In the case of solid-liquid PCM, both melting and crystallisation have to be within the range of

79 charging and discharging temperature of the intended application. The storage capacity which is
80 achieved in a storage unit is not an intrinsic material property but affected by the design of the storage
81 and the conditions given by the application. The expectable maximum storage capacity of a PCM in a
82 defined temperature range is equal to the enthalpy change upon melting or crystallisation in that
83 temperature range and can be determined via calorimetric measurements such as differential scanning
84 calorimetry (DSC) or T-History calorimetry [4]-[7]. DSC samples (~15 μ l) are about 1000 times
85 smaller than T-History samples (~15 ml). Therefore, T-History measurements are favoured over DSC
86 measurements in the case of heterogeneous materials, materials with volume-dependent crystallisation
87 behaviour, and non-congruently melting materials [6]. Experiments in a pilot plant are performed to
88 study the charging and discharging behaviour of even larger amounts of PCM (~150 l, i.e. 10^7 times
89 larger than DSC samples; hereinafter referred to as pilot plant scale). Measurements of such large
90 quantities of PCM are of peculiar interest if the PCM is not encapsulated. In the case of encapsulated
91 PCM, other experiments are required to study their applicability.

92 The common practise is to investigate PCM at one scale, rarely at two scales [6], [7]. In this study,
93 four PCM (RT58, bischofite, D-mannitol, and hydroquinone) were investigated at three scales, namely
94 via DSC, T-History, and at pilot plant scale. In this context, the question arises how to deal with
95 different enthalpy measurements [8]. In literature, the melting enthalpy is usually assigned to a single
96 temperature without indicating the temperature range considered for evaluation. In very few instances,
97 the enthalpy change within a defined temperature range is stated [7]. In this work,
98 enthalpy-temperature plots are demonstrated to be advantageous compared with tabular enthalpy
99 changes within defined temperature ranges in order to compare measurements under different
100 conditions at different scales [9]. The novelty of the paper is that it is the first time such a comparison
101 is done in a consistent way. Preliminary results of this study were presented at a conference [10].

102

103 **2. Materials and methods**

104 *2.1. Materials*

105 For this study, materials were selected which have been investigated recently in the pilot plant test

106 facility of the University of Lleida. RT58 is a commercial paraffin which has been proposed for
 107 domestic hot water applications [11]. Bischofite is a mineral which precipitates in the evaporation
 108 ponds during the potassium chloride and lithium carbonate production process in Salar de Atacama,
 109 Chile. The main component of this by-product, about 95 wt%, is $\text{MgCl}_2 \cdot 6\text{H}_2\text{O}$ [12]-[14]. D-mannitol
 110 and hydroquinone are organic PCM which have been studied as solar thermal storage materials
 111 [15]-[21].

112 In the case of bischofite, which is naturally of technical grade, and RT58, a commercial PCM,
 113 materials of the same batch, i.e. of the same grade, were investigated at all three scales. It was not
 114 possible to carry out measurements of technical grade D-mannitol and hydroquinone from the same
 115 supplier via DSC and T-History, because D-mannitol and hydroquinone were not available anymore at
 116 the time of the laboratory scale measurements. Specifications of the investigated materials are given in
 117 Table 1. Indicated melting temperatures T_m and purities are provided by the suppliers.

118

119 **Table 1**

120 Specifications of investigated PCM as given by suppliers.

| Material | Material class | Formula | T_m (°C) | Supplier | Purity (wt%) |
|---------------------------|----------------|--|------------|------------|-----------------|
| RT58 | Paraffin | n/s | 53 – 59 | Rubitherm | n/s |
| Bischofite | Salt hydrate | $\text{MgCl}_2 \cdot 6\text{H}_2\text{O}$ ^c | n/s | SALMAG | 95 ^c |
| D-mannitol ^a | Sugar alcohol | $\text{C}_6\text{H}_{14}\text{O}_6$ | 167 – 169 | Alfa Aesar | 99 |
| D-mannitol ^b | “ | “ | n/s | QUIMIVITA | 96 |
| Hydroquinone ^a | Phenol | $\text{C}_6\text{H}_6\text{O}_2$ | 172 | Merck | ≥99.5 |
| Hydroquinone ^b | “ | “ | n/s | QUIMIVITA | 95 |

121 ^a measured via DSC and T-History, ^b measured at pilot plant scale, ^c main component, n/s = not specified

122

123 Samples were prepared using the solid substances as purchased. DSC and T-History samples were
 124 prepared with a weighing accuracy of 0.01 mg and pilot plant samples with a weighing accuracy of
 125 100 g. Sample masses of investigated materials are listed in Table 2.

126

127

128

129

130

131 **Table 2**

132 Sample masses used in DSC and T-History measurements and at pilot plant scale.

| Material | m_{DSC} (mg) | $m_{\text{T-History}}$ (g) | $m_{\text{pilot plant}}$ (kg) |
|--------------|-----------------------|----------------------------|-------------------------------|
| RT58 | 12.35 | 9.61 | 108 |
| Bischofite | 11.57 | 17.11 | 204 |
| D-mannitol | 4.76 | 11.07 | 160 |
| Hydroquinone | 9.86 | 15.36 | 170 |

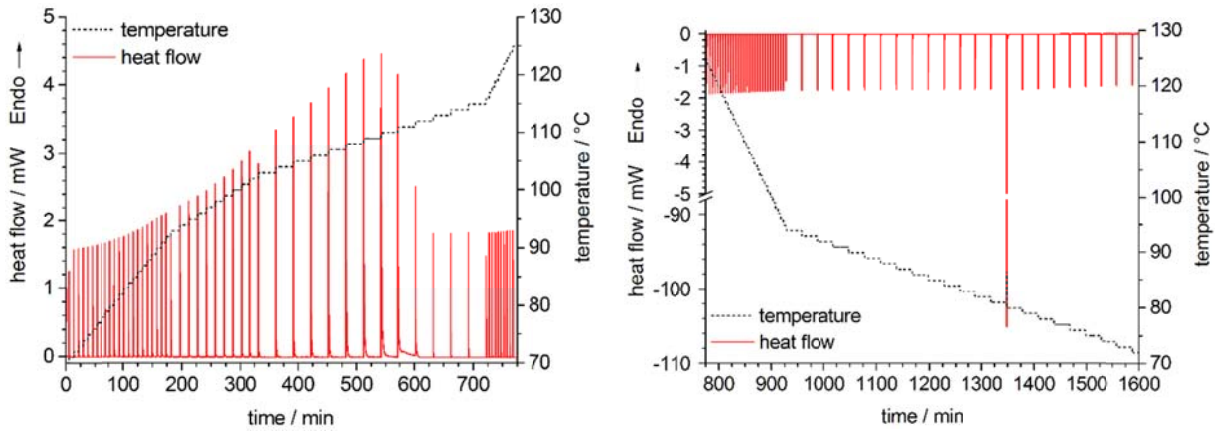
133

134 2.2. DSC measurements

135 DSC measurements were carried out at ZAE Bayern using a TA Q2000 heat-flux DSC device
136 which was calibrated with indium as recommended by TA Instruments. The sufficiency of the single
137 point indium calibration was verified via additional measurements of gallium and biphenyl in terms of
138 temperature, and distilled water in terms of enthalpy. The accuracy of enthalpy curves determined with
139 this DSC device has been approved in various comparative studies, such as the round robin test of
140 octadecane within IEA SHC Task 42 / ECES Annex 24 and its continuation IEA SHC Task 42 / ECES
141 Annex 29 [22]. Based on the participation in Annex 24 / 29 and the authors' experience, the enthalpy
142 can be measured via this DSC device with an accuracy of $\pm 5\%$. A constant stream of nitrogen
143 ($50 \text{ ml} \cdot \text{min}^{-1}$) was applied as flushing gas during the entire DSC measurements. Hermetically sealed
144 alodined aluminium crucibles were used for DSC measurements.

145 According to the RAL testing regulations (RAL German Institute for Quality Assurance and
146 Certification of PCM Gütegemeinschaft e.V. [23]), a temperature resolution of 1 K is required to
147 indicate the enthalpy change upon melting and crystallisation. Therefore, DSC step measurements
148 with temperature steps of 1 K were performed in this study. Using a heat-flux DSC in isothermal step
149 mode, the ambience of PCM (placed inside a crucible) and reference (an empty crucible) is heated up
150 and cooled down stepwise in given temperature intervals [24]-[27]. The PCM temperature follows the
151 temperature step of the DSC oven with some time delay. Before the next temperature step can follow,
152 the measured heat flow signal has to decrease to zero. The temperature resolution of the acquired data
153 is equal to the step size. The heat flow signal of each step is integrated using a linear baseline and the
154 cumulative sum is calculated for the determination of enthalpy curves.

155 Typical data of a DSC step measurement is shown in Fig. 1. To measure the melting and
 156 crystallisation curve of bischofite which melts around 105 °C, the ambient temperature was increased
 157 stepwise from 70 °C to 125 °C and decreased stepwise from 125 °C to 70 °C, respectively.
 158

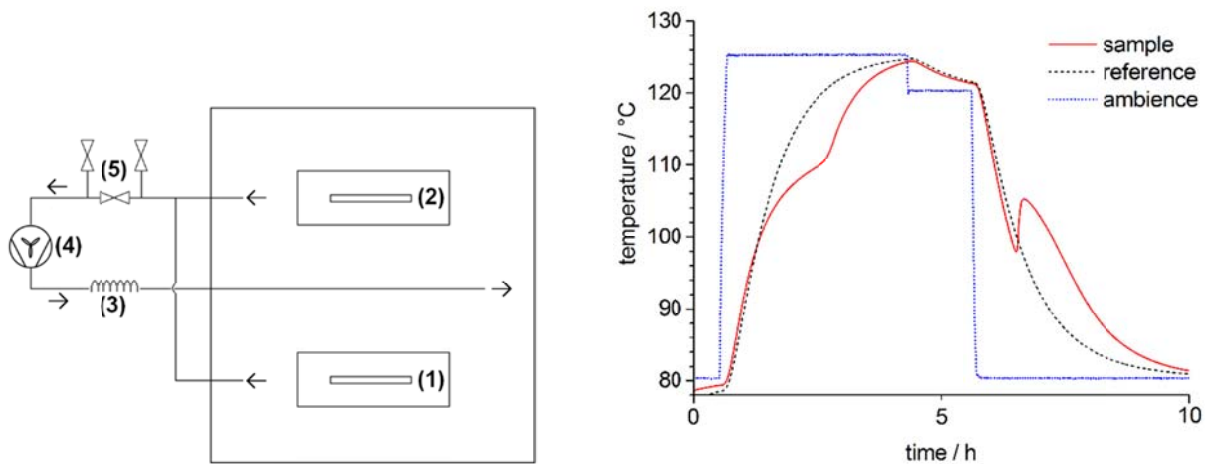


159
 160 **Fig. 1.** DSC step measurement of bischofite consisting of a heating run (left) and a cooling run (right).
 161

162 **2.3. T-History measurements**

163 T-History measurements were performed with a calorimeter which was designed and built at ZAE
 164 Bayern [28]. A top-view sketch of the calorimeter is shown in Fig. 2, left.

165



166
 167 **Fig. 2.** Top-view sketch of the T-History calorimeter (left): PCM with insulation (1), reference with insulation (2). Further
 168 details are given in [4]; Temperature – time data of bischofite (red solid line), reference (black dashed line), and ambience
 169 (blue dotted line) during a T-History measurement (right).

170
171
172
173
174
175
176
177
178
179
180
181
182
183
184
185
186
187
188
189

In a T-History measurement, the PCM is exposed to constant charging / discharging temperatures instead of stepwise temperature increases or temperature ramps, as it is done in DSC measurements. The T-History calorimeter at ZAE Bayern can be used for the determination of enthalpy curves of samples of about 15 ml between 40 °C and 200 °C and was calibrated with indium, electrolytic copper, and three organic PCM [4]. Further information about the T-History method and technical details of the applied instrument can be found in literature [4], [26], [29], [30].

An example for typical temperature-time data measured via T-History is shown in Fig. 2, right. For the measurement of enthalpy curves of bischofite, the ambient temperature was changed from 80 °C to 125 °C in the case of melting, and from 120 °C to 80 °C in the case of crystallisation. Different temperature steps are required for heating and cooling due to the supercooling of bischofite and the fact that the first 15-30 minutes of each heating or cooling segment cannot be evaluated due to an unstable ambient temperature.

2.4. Measurements at pilot plant scale

The pilot plant facility used to experimentally test PCM was designed and built at the University of Lleida [13], [18]. This equipment consists of three main parts: the heating system, the cooling system, and the storage system (Fig. 3).

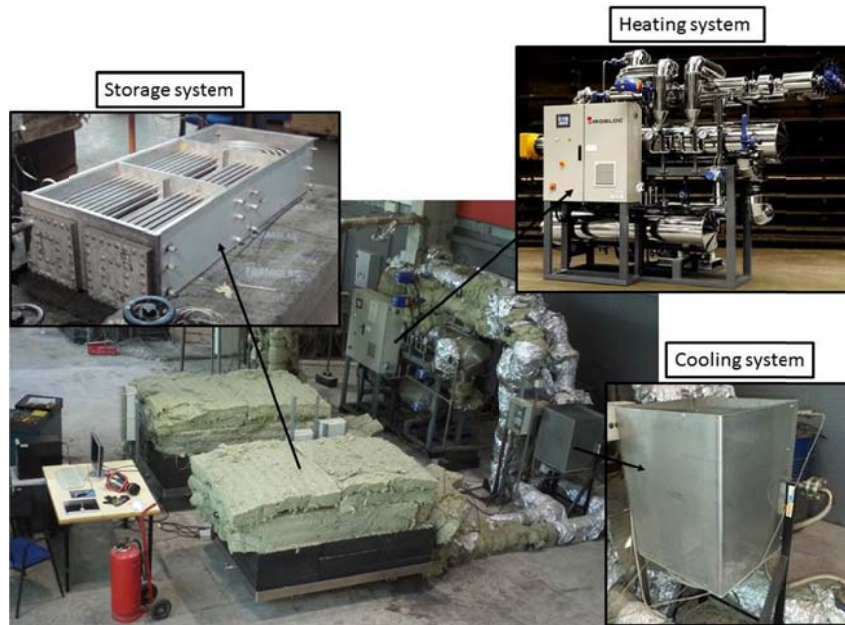


Fig. 3. Pilot plant facility built at the University of Lleida [13].

190

191

192

193

194

195

196

197

198

199

200

201

202

203

204

205

206

207

208

The heating system consists of a 20 kW_{th} electrical boiler supplied by the Pirobloc Company. The boiler heats up the heat transfer fluid (HTF) acting as the heating energy source during a charging process in a real installation. HTF flow rates between 0.3-3 m³·h⁻¹ can be applied. The cooling system is based on a 20 kW_{th} air-HTF heat exchanger (AHE) which simulates the energy consumption by the user during a discharging process. The AHE was designed and built at the University of Lleida and it is based on the cross-flow heat exchanger concept. The heat exchange is carried out by circulating air at ambient temperature with a flow rate of 1800 m³·h⁻¹ through a set of 50 fins and 56 tubes arranged in zigzags, inside which the HTF circulates.

The tank used to store the PCM and to realise the energy exchange between HTF and PCM consists of a shell-and-tube heat exchanger made of stainless steel. The insulated tank vessel has a volume of 154 l (145 l of which can be filled with PCM) and houses 49 tubes with an average length of 2.49 m. To have accurate data on the phase change temperatures of the PCM under investigation, 19 Pt100 temperature sensors with an accuracy of ±0.1 °C are installed at different positions inside the tank. In the figures providing the measured data, the output of a sensor from the middle of the tank was considered as the PCM temperature. Due to this loss in temperature precision, only the overall amount of energy stored upon charging or discharging the storage tank can be calculated. Thus, the

209 temperature accuracy of enthalpy determination at pilot plant scale is lower compared with the two
210 other calorimetric instruments which are operated and calibrated in a way that highly accurate
211 enthalpy-temperature plots can be determined. Instead, the main objective of pilot plant measurements
212 is to characterize the PCM together with the storage tank in terms of the storage capacity in a
213 temperature range covering the entire phase transition, the achieved power output, and the stability
214 upon repeated thermal cycling. Further information on the temperature measurement and data
215 evaluation of measurements at pilot plant scale are given in literature [13].

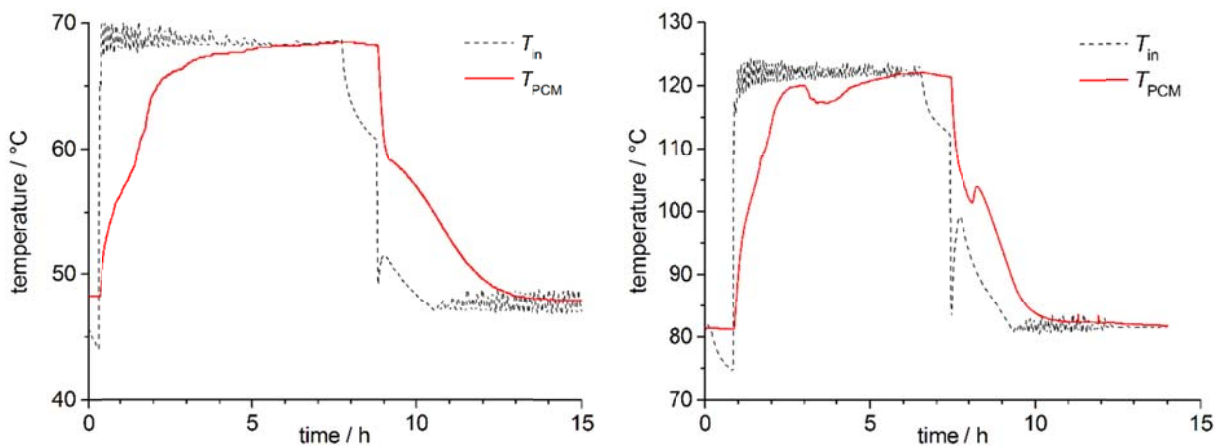
216

217 3. Results and discussion

218 3.1. Temperature-time data measured at pilot plant scale

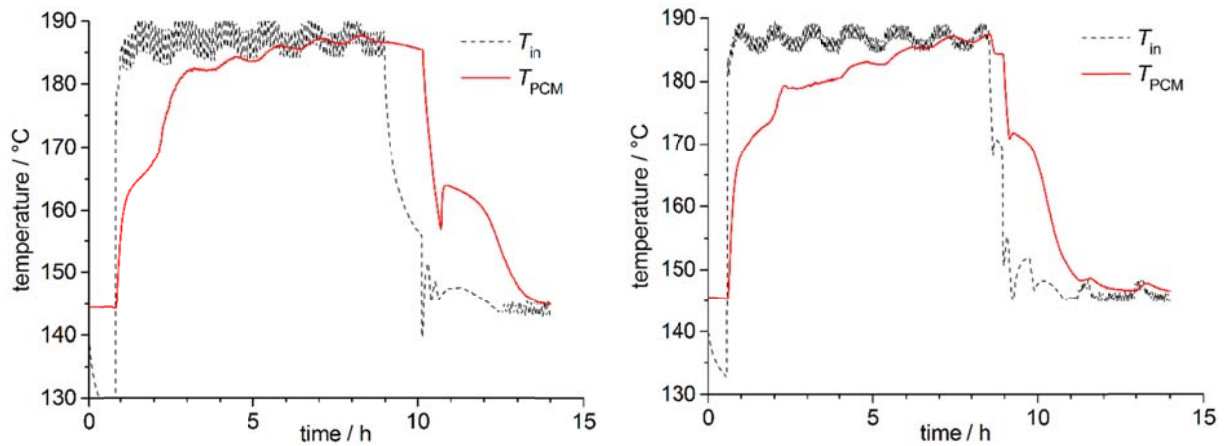
219 To measure the melting and crystallisation of RT58, the tank inlet temperature T_{in} was changed
220 from 48 °C to 68 °C and vice versa, respectively. In the case of bischofite, 80 °C and 120 °C turned
221 out to be appropriate, and for both D-mannitol and hydroquinone, 145 °C and 187 °C were applied as
222 inlet temperatures. The temperature-time data measured at pilot plant scale for one heating-cooling
223 cycle is shown in Fig. 4 (RT58 and bischofite) and Fig. 5 (hydroquinone and D-mannitol). The
224 oscillation observed on the HTF temperature profile is due to the intrinsic configuration of the
225 electrical heater [13].

226



227

228 **Fig. 4.** Temperature-time data of melting and crystallisation of RT58 (left) and bischofite (right) at pilot plant scale. Tank inlet
 229 (T_{in}) and PCM (T_{PCM}) temperatures are plotted with dashed and solid lines, respectively.
 230



231
 232 **Fig. 5.** Temperature-time data of melting and crystallisation of D-mannitol (left) and hydroquinone (right) at pilot plant scale.
 233 Tank inlet (T_{in}) and PCM (T_{PCM}) temperatures are plotted with dashed and solid lines, respectively.
 234

235 *3.2. Comparison of measurements via DSC, T-History, and at pilot plant using enthalpy-temperature*
 236 *plots*

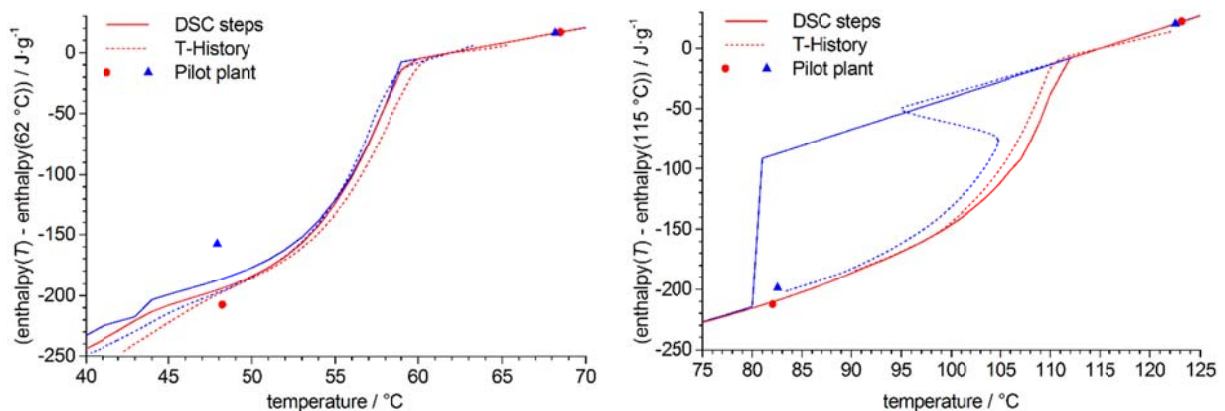
237 In this work, the results of the calorimetric measurements via DSC, T-History, and at pilot plant
 238 scale are given as enthalpy-temperature plots. Due to the different evaluation procedures,
 239 enthalpy-temperature plots are the only common graphical representation suitable for these methods.
 240 In the case of DSC and T-History, the measured results are given as continuous enthalpy curves $h(T)$.
 241 At pilot plant scale, the total amount of energy stored / released upon melting or crystallization within
 242 a certain temperature range is calculated, which can be translated into enthalpy stored / released per kg
 243 PCM. Therefore, in the enthalpy-temperature plots, pilot plant measurements are indicated with two
 244 data points for heating and two data points for cooling.

245 If the thermal connection between PCM and DSC crucible or PCM and T-History sample container
 246 changes after first melting, the data of the first cycle differs from succeeding cycles. Thus, only the
 247 second cycle of each measurement is plotted and used to determine a suitable temperature range and
 248 the corresponding enthalpy changes therein. The fact that the first cycle needs to be disregarded when

249 measuring enthalpy curves with DSC is known from literature. However, this conclusion is not as well
250 stated and known in the case of the T-History method. As observed in the experiments, the first cycle
251 should also be disregarded. In the case of measurements at pilot plant scale, the stabilization of the
252 PCM might need more than one cycle.

253 Red lines represent heating and blue lines represent cooling curves. Enthalpy curves measured via
254 DSC and T-History are plotted with solid and dashed lines, respectively. Red circles and blue triangles
255 indicate the enthalpy changes measured at pilot plant scale upon melting and crystallisation,
256 respectively. In the plots, enthalpy curves measured via DSC and T-History and enthalpy changes
257 measured at pilot plant scale were shifted to a common zero point located in the liquid state, which is
258 denoted in the label of the enthalpy axis. Shifting to a common zero point in the liquid state is
259 reasonable since the liquid state can be considered as identical from one cycle to another. The results
260 for RT58 and bischofite are shown in Fig. 6 and the results for D-mannitol and hydroquinone in Fig. 7.

261

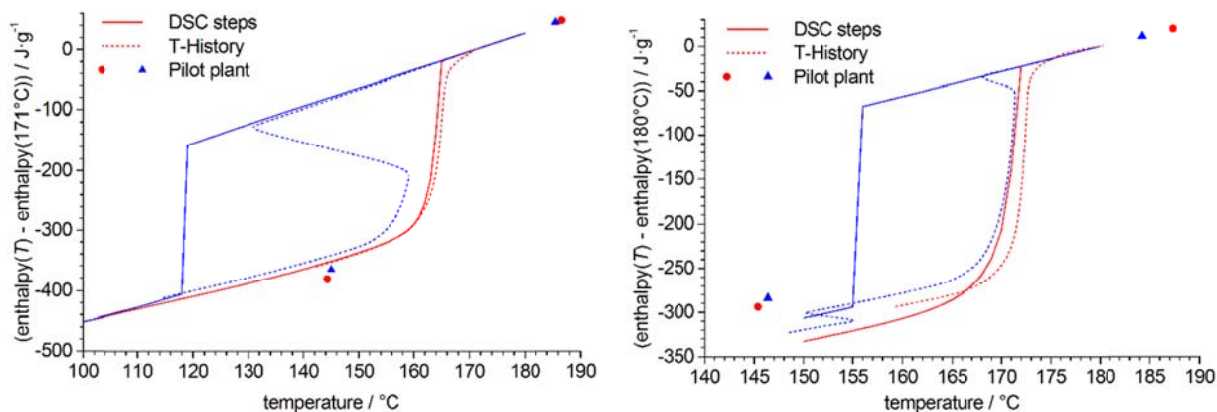


262

263 **Fig. 6.** Enthalpy curves of RT58 (left) and bischofite (right) measured via DSC in step mode (solid line) and T-History (dashed
264 line). Red circles and blue triangles indicate the enthalpy changes measured at pilot plant scale upon melting and
265 crystallisation, respectively.

266

267



268

269 **Fig. 7.** Enthalpy curves of D-mannitol (left) and hydroquinone (right) measured via DSC in step mode (solid line) and
 270 T-History (dashed line). Red circles and blue triangles indicate the enthalpy changes measured at pilot plant scale upon
 271 melting and crystallisation, respectively.

272

273 The enthalpy curves measured via DSC and T-History indicate a volume-independent melting and
 274 crystallisation behaviour of RT58. Melting and crystallisation occur within a temperature range
 275 matching the specifications of the supplier (53–59 °C). In the case of bischofite, D-mannitol, and
 276 hydroquinone, a significant degree of supercooling is observed in DSC step measurements. After
 277 nucleation, the crystallisation evolves in a single temperature step. The supercooling of bischofite,
 278 D-mannitol, and hydroquinone in T-History measurements is reduced compared to DSC results. At
 279 pilot plant scale, a further reduction of the degree of supercooling compared to T-History data is
 280 observed (cf. Fig. 4 and Fig. 5). This trend was expected from own experience and literature [2], [6].

281 The enthalpy change of RT58 during the crystallisation at pilot plant scale is comparably low.
 282 Enthalpy curves of hydroquinone upon cooling measured via T-History indicate a second transition
 283 upon cooling between 155 °C and 150 °C (cf. Fig. 7, right), as described in a previous publication [6].
 284 This additional transition was not observed in DSC or pilot plant measurements and might contribute
 285 to the comparably low enthalpy changes determined at pilot plant scale. Except for the crystallisation
 286 of RT58 at pilot plant scale and influence of the second transition of hydroquinone,
 287 enthalpy-temperature plots upon melting and crystallisation measured at different sample scales show
 288 a reasonable agreement.

289

290 *3.3. Tabular comparison of enthalpy changes in defined temperature ranges*

291 In order to show how difficult an evaluation of measurements under different conditions would
 292 have been without using enthalpy-temperature plots, enthalpy changes upon melting and
 293 crystallization within defined temperature ranges measured at the three scales are compared in Table 3.

294

295 **Table 3**

296 Enthalpy changes upon melting $\Delta h_{\Delta T_m}$ and crystallisation $\Delta h_{\Delta T_c}$ within defined temperature ranges ΔT_m and ΔT_c measured via
 297 DSC, T-History, and at pilot plant scale.

| | RT58 | | | | Bischofite | | | |
|-------------|----------------------|---|----------------------|---|----------------------|---|----------------------|---|
| | ΔT_m (°C) | $\Delta h_{\Delta T_m}$ (J·g ⁻¹) | ΔT_c (°C) | $\Delta h_{\Delta T_c}$ (J·g ⁻¹) | ΔT_m (°C) | $\Delta h_{\Delta T_m}$ (J·g ⁻¹) | ΔT_c (°C) | $\Delta h_{\Delta T_c}$ (J·g ⁻¹) |
| DSC | 52-62 | 167 | 52-62 | 162 | 75-115 | 228 | 75-115 | 227 |
| T-History | 52-62 | 170 | 52-62 | 167 | 90-115 | 186 | 90-115 | 183 |
| Pilot plant | 48-68 | 224 | 48-68 | 173 | 82-123 | 235 | 83-123 | 220 |
| | D-mannitol | | | | Hydroquinone | | | |
| | ΔT_m (°C) | $\Delta h_{\Delta T_m}$ (J·g ⁻¹) | ΔT_c (°C) | $\Delta h_{\Delta T_c}$ (J·g ⁻¹) | ΔT_m (°C) | $\Delta h_{\Delta T_m}$ (J·g ⁻¹) | ΔT_c (°C) | $\Delta h_{\Delta T_c}$ (J·g ⁻¹) |
| DSC | 115-165 | 400 | 115-165 | 396 | 150-180 | 333 | 150-180 | 307 |
| T-History | 131-171 | 389 | 131-171 | 375 | 160-180 | 292 | 160-180 | 278 |
| Pilot plant | 144-187 | 428 | 145-186 | 409 | 145-187 | 314 | 146-184 | 295 |

298

299 The expectable maximum storage capacity of a PCM in a defined temperature range is equal to
 300 the enthalpy change in that range. Therefore, the enthalpy changes upon melting ($\Delta h_{\Delta T_m}$) and
 301 crystallisation ($\Delta h_{\Delta T_c}$) were determined within temperature ranges ΔT_m and ΔT_c , respectively. In the
 302 case of DSC and T-History measurements, temperature ranges were chosen which cover the entire
 303 phase change upon melting and crystallisation according to measured data (cf. Fig. 6 and Fig. 7). At
 304 pilot plant scale, only the overall amount of energy stored upon charging / discharging the storage tank
 305 is calculated enthalpy. Therefore, changes upon melting and crystallisation were evaluated considering
 306 a temperature interval which is approximately the range between the initial and final storage tank inlet
 307 temperatures (cf. Fig. 4 and Fig. 5). In the case of D-mannitol (cf. Fig. 7, left), the enthalpy curve
 308 measured via T-History upon heating was extrapolated to lower temperatures to determine the

309 enthalpy change. Thus, due to the different measuring methods and their specific evaluation
310 procedures, the temperature ranges ΔT_m and ΔT_c applied to calculate $\Delta h_{\Delta T_m}$ and $\Delta h_{\Delta T_c}$ vary
311 significantly.

312 Using a tabular comparison as shown in Table 3, it is not clear if the differences in $\Delta h_{\Delta T_m}$ and
313 $\Delta h_{\Delta T_c}$ between the different sample scales / measuring methods arise from the different temperature
314 ranges considered for evaluation or from an actual deviation in the measured enthalpy-temperature
315 data. For example, in the case of bischofite, enthalpy-temperature plots upon melting show a very
316 good agreement (cf. Fig. 6, right). Contrary, indicated enthalpy changes upon melting, $\Delta h_{\Delta T_m}$, in Table
317 3 exhibit a deviation of up to 21% comparing T-History data with measurements at pilot plant scale.

318

319 **4. Conclusions**

320 Four PCM from different material classes (RT58, bischofite, D-mannitol, and hydroquinone) were
321 investigated at three sample scales, namely via DSC, T-History, and at pilot plant scale.

322 To compare the enthalpy changes measured at different scales and under different conditions,
323 enthalpy-temperature plots were demonstrated to be advantageous compared with tabular enthalpy
324 changes within defined temperature ranges. Since the temperature range chosen to calculate the
325 expectable maximum storage capacity differs from method to method due to their different data
326 evaluation procedures, the comparison becomes difficult even if the temperature ranges are reported
327 next to the calculated enthalpy change. It is not clear if possible differences between the different
328 sample scales / measuring methods arise from the different temperature ranges considered for the
329 evaluation or from an actual deviation in the measured enthalpy-temperature data.

330 Except for the crystallisation of RT58 at pilot plant scale and influence of a second transition of
331 hydroquinone, enthalpy-temperature plots upon melting and crystallisation measured at different
332 sample scales show a reasonable agreement. However, relying on a tabular comparison of enthalpy
333 changes within defined temperature ranges, this conclusion cannot be drawn.

334

335 **Acknowledgements**

336 The work of ZAE Bayern was part of the project EnFoVerM and was supported by the German
337 Federal Ministry for Economic Affairs and Energy under the project code 0327851D.

338 The work at the University of Lleida is partially funded by the Spanish government
339 (ENE2011-22722, ENE2015-64117-C5-1-R (MINECO/FEDER) and ULLE10-4E-1305). The authors
340 would like to thank the Catalan Government for the quality accreditation given to their research group
341 GREA (2014 SGR 123). GREA is a certified agent TECNIO in the category of technology developers
342 from the Government of Catalonia. The research leading to these results has received funding from the
343 European Union's Seventh Framework Programme (FP7/2007-2013) under grant agreement n°
344 PIRSES-GA-2013-610692 (INNOSTORAGE) and from the European Union's Horizon 2020 research
345 and innovation programme under grant agreement No 657466 (INPATH-TES). The authors want also
346 to thank the collaboration of Antoni Gil from Massachusetts Institute of Technology (USA), Eduard
347 Oró from Catalonia Institute for Energy Research (Spain), and Jaume Gasia and Gerard Peiró from
348 University of Lleida (Spain). Laia Miró would like to thank the Spanish Government for her research
349 fellowship (BES-2012-051861).

350 The work of the University of Antofagasta was supported by FONDAP SERC-Chile (grant N°
351 15110019), and the Education Ministry of Chile Grant PMI ANT 1201. Authors thank the SALMAG
352 Company for providing of bischofite. Andrea Gutierrez would like to acknowledge to the Ministry of
353 Education of Chile her doctorate scholarship ANT 1106 and CONICYT/PAI N° 7813110010.

354

355 **References**

- 356 [1] L.F. Cabeza, A. Castell, C. Barreneche, A. de Gracia, A.I. Fernández, Materials used as PCM in thermal energy
357 storage in buildings: A review, *Renew. Sust. Energ. Rev.* 15 (2011) 1675-1695.
- 358 [2] H. Mehling, L.F. Cabeza, *Heat and cold storage with PCM – An up to date introduction into basics and applications*,
359 first ed., Springer, Berlin, 2008.
- 360 [3] M.M. Kenisarin, Thermophysical properties of some organic phase change materials for latent heat storage. A
361 review, *Sol. Energy* 107 (2014) 553-575.
- 362 [4] C. Rathgeber, H. Schmit, P. Hennemann, S. Hiebler, Calibration of a T-History calorimeter to measure enthalpy
363 curves of phase change materials in the temperature range from 40 to 200 °C, *Meas. Sci. Technol.* 25 (2014)
364 035011(10pp).

- 365 [5] C. Rathgeber, H. Schmit, P. Hennemann, S. Hiebler, Investigation of pinacone hexahydrate as phase change
366 material for thermal energy storage around 45 °C, *Appl. Energ.* 136 (2014) 7-13.
- 367 [6] C. Rathgeber, L. Miró, L.F. Cabeza, S. Hiebler, Measurement of enthalpy curves of phase change materials via
368 DSC and T-History: When are both methods needed to estimate the behaviour of the bulk material in applications?,
369 *Thermochim. Acta* 596 (2014) 79-88.
- 370 [7] H. Schmit, C. Rathgeber, P. Hennemann, S. Hiebler, Three-step method to determine the eutectic composition of
371 binary and ternary mixtures, *J. Therm. Anal. Calorim.* 117 (2) (2014) 595-602.
- 372 [8] H. Mehling, C. Barreneche, A. Solé, L.F. Cabeza, The connection between the heat storage capability of PCM as a
373 material property and their performance in real scale applications, *Journal of Energy Storage* 13 (2018) 35-39.
- 374 [9] E. Günther, S. Hiebler, H. Mehling, R. Redlich, Enthalpy of Phase Change Materials as a Function of Temperature:
375 Required Accuracy and Suitable Measurement Methods, *Int. J. Thermophys.* 30 (2009) 1257-1269.
- 376 [10] C. Rathgeber, H. Schmit, L. Miró, L.F. Cabeza, A. Gutierrez, et al., Analysis of supercooling of phase change
377 materials with increased sample size – Comparison of measurements via DSC, T-History and at pilot plant scale,
378 *Proc. of Greenstock 2015 – 13th International Conference on Energy Storage*, Beijing, China, 2015.
- 379 [11] J. Gasia, L. Miró, A. de Gracia, C. Barreneche, L.F. Cabeza, Experimental evaluation of a paraffin as phase change
380 material for thermal energy storage in laboratory equipment and in a shell-and-tube heat exchanger, *Appl. Sci.* 6
381 (2016) 112.
- 382 [12] S.N. Ushak, A. Gutierrez, H. Galleguillos, A.G. Fernandez, L.F. Cabeza, et al., Thermophysical characterization of
383 a by-product from the non-metallic industry as inorganic PCM, *Sol. Energy Mater. Sol. Cells* 132 (2015) 385–391.
- 384 [13] J. Gasia, A. Gutierrez, G. Peiró, L. Miró, M. Grágeda, et al., Thermal performance evaluation of bischofite at pilot
385 plant scale, *Appl. Energ.* 155 (2015) 826-833.
- 386 [14] A. Gutierrez, S.N. Ushak, H. Galleguillos, A.G. Fernandez, L.F. Cabeza, et al., Use of polyethylene glycol for the
387 improvement of the cycling stability of bischofite as thermal energy storage material, *Appl. Energ.* 154 (2015)
388 616-621.
- 389 [15] C. Barreneche, A. Gil, F. Sheth, A.I. Fernández, L.F. Cabeza, Effect of d-mannitol polymorphism in its thermal
390 energy storage capacity when it is used as PCM, *Sol. Energy* 94 (2013) 344-351.
- 391 [16] A.J. Gallego, A. Ruíz-Pardo, A. Cerezuela-Parish, J. Sánchez, C. Martín-Macareno, et al., Mathematical modeling
392 of a PCM storage tank in a solar cooling plant, *Sol. Energy* 93 (2013) 1-10.
- 393 [17] A. Gil, C. Barreneche, P. Moreno, C. Solé, A.I. Fernández, et al., Thermal behaviour of D-mannitol when used as
394 PCM: Comparison of results obtained by DSC and in a thermal energy storage unit at pilot plant scale, *Appl. Energ.*
395 111 (2013) 1107-1113.
- 396 [18] A. Gil, E. Oró, G. Peiró, S. Álvarez, L.F. Cabeza, Material selection and testing for thermal energy storage in solar
397 cooling, *Renew. Energ.* 57 (2013) 366-371.

- 398 [19] A. Gil, E. Oró, L. Miró, G. Peiró, Á. Ruiz, et al., Experimental analysis of hydroquinone used as phase change
399 material (PCM) to be applied in solar cooling refrigeration, *Int. J. Refrig.* 39 (2014) 95-103.
- 400 [20] Z. Fan, C.A. Infante Ferreira, A.H. Mosaffa, Numerical modelling of high temperature latent heat thermal storage
401 for solar application combining with double-effect H₂O/LiBr absorption refrigeration system, *Sol. Energy* 110
402 (2014) 389-409.
- 403 [21] A. Solé, H. Neumann, S. Niedermaier, I. Martorell, P. Schossig P, et al., Stability of sugar alcohols as PCM for
404 thermal energy storage, *Sol. Energy Mater. Sol. Cells* 126 (2014) 125–134.
- 405 [22] Task 42 / Annex 29 “Compact thermal energy storage” <http://task42.iea-shc.org/>, 2017.
- 406 [23] Quality Association PCM (RAL Gütegemeinschaft PCM e. V.),
407 <http://www.pcm-ral.org/pcm/en/quality-testing-specifications-pcm/>, 2017.
- 408 [24] C. Barreneche, A. Solé, L. Miró, I. Martorell, A.I. Fernández, et al., Study on differential scanning calorimetry
409 analysis with two operation modes and organic and inorganic phase change material (PCM), *Thermochim. Acta*
410 553 (2013) 23-26.
- 411 [25] C. Castellón, E. Günther, H. Mehling, S. Hiebler, L.F. Cabeza, Determination of the enthalpy of PCM as a function
412 of temperature using a heat-flux DSC – a study of different measurement procedures and their accuracy, *Int. J.*
413 *Energy Res.* 32 (2008) 1258-1265.
- 414 [26] S. Hiebler, Kalorimetrische Methoden zur Bestimmung der Enthalpie von Latentwärmespeichermaterialien
415 während des Phasenübergangs, PhD Thesis, Technische Universität München, Garching, 2007.
- 416 [27] G.W.H. Höhne, W.F. Hemminger, H.J. Flammersheim, *Differential Scanning Calorimetry*, second ed., Springer,
417 Berlin, 1989.
- 418 [28] C. Rathgeber, M. Himpel, S. Hiebler, A new T-history calorimeter for phase change materials in the temperature
419 range 50 °C – 200 °C, *Proc. of Innostock – 12th International Conference on Energy Storage*, Lleida, Spain, 2012.
- 420 [29] A. Lázaro, E. Günther, H. Mehling, S. Hiebler, J.M. Marín, et al., Verification of a T-history installation to measure
421 enthalpy versus temperature curves of phase change materials, *Meas. Sci. Technol.* 17 (2006) 2168-2174.
- 422 [30] J.M. Marín, B. Zalba, L.F. Cabeza, H. Mehling, Determination of enthalpy-temperature curves of phase change
423 materials with the temperature-history method: improvement to temperature dependent properties, *Meas. Sci.*
424 *Technol.* 14 (2003) 184-189.